Cell Reports
Report

Cell PRESS
Open ACCESS

Localization-Dependent and -Independent Roles of SLX4 in Regulating Telomeres

Jamie S.J. Wilson,[1] Agueda M. Tejera,[2] Dennis Castor,[1] Rachel Toth,[1] Maria A. Blasco,[2] and John Rouse[1,*]
[1]MRC Protein Phosphorylation and Ubiquitylation Unit, College of Life Sciences, University of Dundee, Dundee DD1 5EH, Scotland, UK
[2]Spanish National Cancer Research Centre (CNIO), Molecular Oncology Program, Madrid E-28029, Spain
*Correspondence: j.rouse@dundee.ac.uk
http://dx.doi.org/10.1016/j.celrep.2013.07.033

SUMMARY

SLX4, a scaffold for structure-specific DNA repair nucleases, is important for several types of DNA repair. Many repair proteins bind to sites of DNA damage, resulting in subnuclear "foci," but SLX4 forms foci in human cells even without DNA damage. Using several approaches, we show that most, but not all, SLX4 foci localize to telomeres in a range of human cell lines irrespective of the mechanisms used to maintain telomere length. The SLX1 Holliday-junction-processing enzyme is recruited to telomeres by SLX4, and SLX4, in turn, is recruited by a motif that binds to the shelterin subunit TRF2 directly. We also show that TRF2-dependent recruitment of SLX4 prevents telomere damage. Furthermore, SLX4 prevents telomere lengthening and fragility in a manner that appears to be independent of telomere association. These findings reveal that SLX4 plays multiple roles in regulating telomere homeostasis.

INTRODUCTION

SLX4 is a scaffold protein that binds to three DNA repair endonucleases, MUS81-EME1, XPF-ERCC1, and SLX1 (Andersen et al., 2009; Fekairi et al., 2009; Muñoz et al., 2009; Saito et al., 2009; Svendsen et al., 2009). The SLX4 complex is required for the efficient repair of DNA interstrand crosslinks (ICLs), (Fekairi et al., 2009; Muñoz et al., 2009; Svendsen et al., 2009), and the available evidence strongly suggests a role in processing DNA recombination intermediates during ICL repair. The importance of SLX4 for ICL repair was underscored by the findings that biallelic mutations in SLX4 in humans causes Fanconi anemia (FA) (Kim et al., 2011; Stoepker et al., 2011).

Many DNA repair proteins form subnuclear "foci" at sites of DNA damage, but SLX4 overexpressed in epitope-tagged form localizes to subnuclear foci even without DNA damage (Svendsen et al., 2009). It was suggested that these foci correspond to telomeres, regions of repetitive DNA at chromosome ends, which protect the ends from degradation (Svendsen et al., 2009). Telomeres terminate in an overhang that is thought to invade adjacent duplex telomeric repeats to form a telomeric (T) loop so that the chromosome ends are not perceived as DNA breaks. An additional layer of telomere protection is afforded by a multiprotein complex called shelterin, that binds to telomeric DNA (Palm and de Lange, 2008). In normal somatic cells, telomeres shorten with every cell division, and telomere shortening contributes to organismal aging by limiting the proliferative capacity of adult stem cells (Blasco, 2007). In immortalized cells and in cancers, telomere length is maintained by telomerase, a reverse transcriptase that can add telomere repeats with the aid of an associated RNA template (Greider and Blackburn, 1989; Mocellin et al., 2013). Some other immortalized cells, cancer cells, and even normal somatic cells can lengthen telomeres in a telomerase-independent manner using the ALT (*a*lternative *l*engthening of *t*elomeres) pathway, which probably involves recombination (Bryan et al., 1995; Cesare and Reddel, 2010; Neumann et al., 2013).

A number of observations suggest that SLX4 might function at telomeres. First, when overexpressed in a special clone of HeLa cells with abnormally long telomeres SLX4 forms subnuclear foci that colocalize with shelterin (Svendsen et al., 2009). Second, SLX4 was identified in a global screen for proteins that bind telomeres (Déjardin and Kingston, 2009). Third, SLX4 interacts with TRF2 and RAP1 (Muñoz et al., 2009; Svendsen et al., 2009), which are subunits of shelterin. Also, SLX4 promotes telomere cleavage in cells lacking the RTEL1 helicase (Vannier et al., 2012). In *Rtel1*$^{-/-}$ cells, replisomes stall in telomeres leading to cleavage of T loops and the production of extrachromosomal T circles, which is mediated by the SLX4 complex (Vannier et al., 2012). Although these observations link the SLX4 complex to telomeres, it is not known whether endogenous SLX4 localizes at telomeres, if this is applicable in cells that differ in the mechanisms used to maintain telomere length, or how SLX4 is recruited to chromosome ends. Furthermore, in RTEL1-proficient cells it remains to be determined if SLX4 has a physiological role to play in telomere homeostasis. Here, we address these issues.

RESULTS

The Endogenous SLX4 Complex Localizes at Telomeres

We first tested if endogenous SLX4 localizes at telomeres. Using antibodies raised in-house, we found that endogenous SLX4

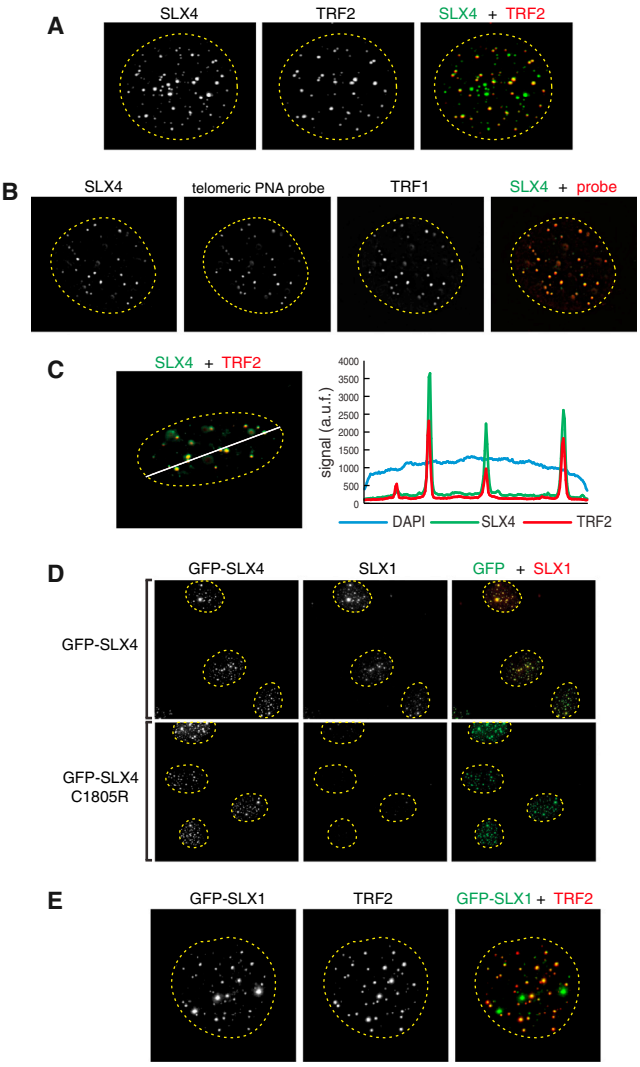

Figure 1. Endogenous SLX4 Complex Localizes at Telomeres in U2OS cells

(A) Indirect immunofluorescence analysis of SLX4 and TRF2 in U2OS cells. Cells were fixed and preextracted, and SLX4 or TRF2 foci were visualized.

(B) U2OS cells were fixed and SLX4 or TRF1 foci were visualized by indirect immunofluorescence. Cells were then fixed again and subjected to FISH analysis with a telomeric PNA probe.

(C) Same as (A), except that a straight line was drawn using OMERO Insight (Allan et al., 2012) through a single Z-section of the nucleus, and the intensity of the SLX4, TRF2, or DAPI signals was quantitated along the length of the line. a.u.f., arbitrary units of fluorescence.

(D) U2OS cells stably expressing GFP-SLX4 or an SLX4 mutant incapable of interacting with SLX1 (GFP-SLX4-C1805R) were fixed, and GFP-SLX4 or SLX1 foci were visualized by indirect immunofluorescence.

(E) Indirect immunofluorescence analysis of SLX1 and TRF2 in U2OS cells stably overexpressing GFP-tagged SLX1.

See also Figure S1.

forms subnuclear foci in U2OS cells without addition of genotoxins (Figure 1A). These foci are specific for SLX4 because they disappeared when cells were transfected with SLX4-specific small interfering RNAs (siRNAs) (Figure S1A). Endogenous SLX4 foci did not appear to be restricted to any particular cell-cycle stage, and they did not increase in number or intensity after exposure of cells to genotoxins (data not shown). To investigate if endogenous SLX4 foci correspond to telomeres, we tested colocalization with subunits of shelterin. Most (around 80%), but not all, endogenous SLX4 foci colocalized with TRF2 in U2OS cells (Figure 1A), and also with TRF1 and with a peptide-nucleic acid (PNA) probe specific for telomeric DNA (Figure 1B). When signal intensity was measured along a straight line in a single Z-section through the nucleus, the peaks corresponding to SLX4 overlap with TRF2 (Figure 1C). It is important to note that, whereas all TRF2 foci in U2OS cells contained SLX4, a proportion of SLX4 foci did not overlap with TRF2 (Figure 1A). These observations indicate that SLX4 is found at all telomeres in U2OS cells, but a proportion of the SLX4 foci do not correspond to telomeres.

SLX4 associates with three separate structure-specific nucleases , XPF-ERCC1, MUS81-EME1, and SLX1. XPF-ERCC1 was previously shown to localize at telomeres (Zhu et al., 2003), and in this light we found that all of the XPF-ERCC1 foci in cells colocalize with SLX4 (Figures S1B and S1D). MUS81-EME1 was also shown to localize at telomeres (Zeng et al., 2009), but only around 5% of U2OS cells show MUS81 foci colocalizing with SLX4 (Figures S1C and S1D). Endogenous SLX1 foci were only barely detectable with our anti-SLX1 antibodies (data not shown). SLX4 controls the stability of SLX1 (Muñoz et al., 2009), and overexpression of a GFP-tagged form of SLX4 increased the levels of endogenous SLX1 (data not shown). Under these conditions, endogenous SLX1 foci could be detected with anti-SLX1 antibodies (Figure 1D), and most of these foci colocalize with TRF2 (data not shown). In contrast, SLX1 foci could not be detected when we overexpressed a mutant form of SLX4 (C1805R) that is incapable of interacting with SLX1 (Figure 1D) (D.C., N. Nair, A.C. Declais, C. Lachaud, R.T., T.J. Macartney, D.M.J. Lilley, J.S.C. Arthur, and J.R., unpublished data). We also found that a GFP-tagged form of SLX1 formed foci that colocalized with TRF2 (Figure 1E). Taken together, these data show that the endogenous SLX4 complex localizes at telomeres.

SLX4 Binds to Telomeres in Cells Differing in Mechanisms of Telomere Length Maintenance

To confirm the association of SLX4 with telomeres, we carried out chromatin immunoprecipitation (ChIP) experiments. Telomeric DNA, but not Alu repeat DNA, was detected in SLX4 immunoprecipitates of U2OS cells using two separate anti-SLX4 antibodies raised in sheep, but not when nonspecific sheep immunoglobulin (Ig) G or anti-CENPA antibodies were used. The ChIP signal in SLX4 precipitates was comparable to the signal in TRF2 precipitates (Figure 2A). We also detected telomeric DNA, but not Alu DNA, in anti-SLX1 immunoprecipitates in U2OS cells (Figure 2B).

Telomere length is maintained by the ALT pathway in U2OS cells, whereas in other cell lines telomere length can be maintained by telomerase (Cesare and Reddel, 2010). ChIP experiments showed that SLX4 associates with telomeric DNA, but not Alu DNA, in A549 and HeLa epithelial cells, two non-ALT cell lines that are telomerase positive (Figures 2C and 2D, left

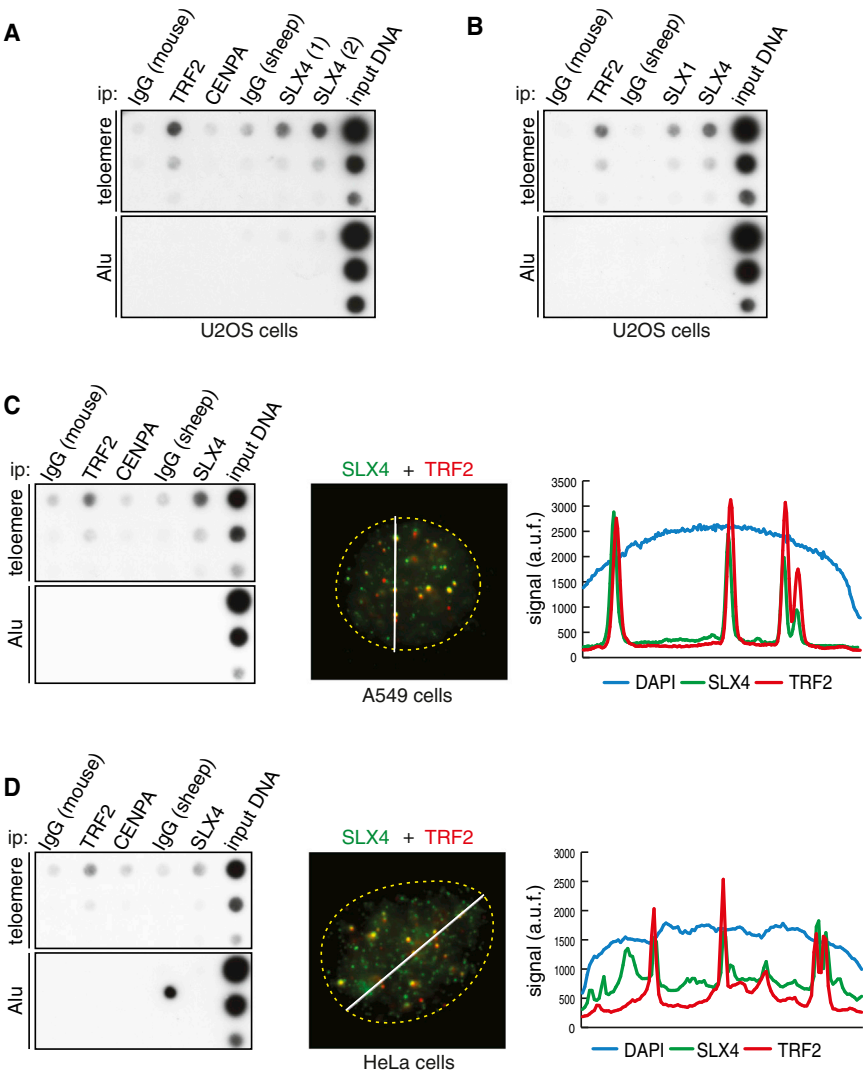

Figure 2. Multiple Approaches Detect SLX4 at Telomeres in Several Human Cell Lines

(A and B) U2OS cells were fixed with formaldehyde, and ChIP analysis was performed with the antibodies indicated. DNA from immunoprecipitates was subjected to 3-fold serial dilutions before spotting onto Hybond N+ and subjected to hybridization with a radioactively labeled telomeric probe or an Alu DNA probe. Input DNA prepared from cell extracts before immunoprecipitation was subjected to similar analysis.

(C) ChIP analysis (left panels) and indirect immunofluorescence analysis of SLX4 or TRF2 foci (middle and right panels) in A549 cells. In the middle panel, a straight line was drawn through a single Z-section of the nucleus, and the intensity of the SLX4, TRF2, or DAPI signals was quantitated along the length of the line (right panel).

(D) Same as (C) except that HeLa cells were used. a.u.f., arbitrary units of fluorescence. In all ChIP experiments, the "input DNA" lane shows 10%, 3%, and 1% of the total DNA in cell extract, respectively.

See also Figure S2.

panels). The ChIP signal in anti-SLX4 immunoprecipitates from these cells was weaker than in U2OS cells, probably because A549 and HeLa cell telomeres are shorter than in U2OS cells (Lee et al., 2008). Nonetheless, the ChIP signal in SLX4 precipitates from A549 and HeLa cells was comparable to the signal in TRF2 precipitates (Figures 2C and 2D, left panels). Furthermore, SLX4 foci in A549 cells and HeLa cells are considerably less intense than in U2OS cells, but a significant proportion of the foci still colocalized with TRF2 (Figures 2C and 2D, middle panels). When signal intensity along an arbitrary track in a single Z-section of the nucleus was quantitated, the peaks corresponding to SLX4 and TRF2 in A549 and HeLa cells demonstrated good overlap (Figures 2C and 2D, right panels). We also observed SLX4 foci in CCL-211 primary lung fibroblasts, and some of these colocalize with TRF1 similar to HeLa cells (Figure S1E). Although a significant proportion of telomeric foci in these cells do not contain SLX4, when signal intensity along an arbitrary track in a single Z-section of the nucleus was quantitated, the peaks corresponding to SLX4 demonstrated reasonably good overlap with TRF1 (Figure S1E). Taken together, these data show that the SLX4 complex localizes at telomeres in a range of human cell lines that differ in the mechanisms used to maintain telomere length.

SLX4 Has a TRF2-Binding Motif

Both subunits of the TRF2-RAP1 shelterin subcomplex were found previously in SLX4 immunoprecipitates (Muñoz et al., 2009; Svendsen et al., 2009). We next sought to determine whether SLX4 is recruited to telomeres by either of these two proteins. Yeast two-hybrid analysis, using XPF as a positive control, revealed that SLX4 binds to TRF2, not RAP1 (Figure 3A), and it seemed likely therefore that SLX4 is recruited to telomeres by TRF2. To investigate this possibility, we sought mutations in SLX4 that abolish the interaction with TRF2, and our search was aided by a previous report describing a motif found in a range of proteins that interact with TRF2 (F/Y-X-L-X-P; Figure 3B) (Chen et al., 2008). Inspection of the primary amino acid sequence of human SLX4 failed to identify a classical TRF2-binding motif (TBM), but we found a TBM-like motif (H^{1020}-X-L^{1022}-X-P^{1024}) in which the first residue (F/Y) is replaced by a histidine residue, which like F and Y contains a planar aromatic ring structure (Figure 3B). This motif in SLX4 lies after the BTB domain in an unstructured region of the protein (Figure 3B, data not shown).

We next tested the effect of mutating the key residues in the putative TBM in human SLX4 on its interaction with TRF2. To this end, U2OS cells were cotransfected with RFP-tagged TRF2 and HA-tagged SLX4 wild-type or HA-SLX4 in which H1020, L1022, or P1024 were mutated to alanine. Whereas

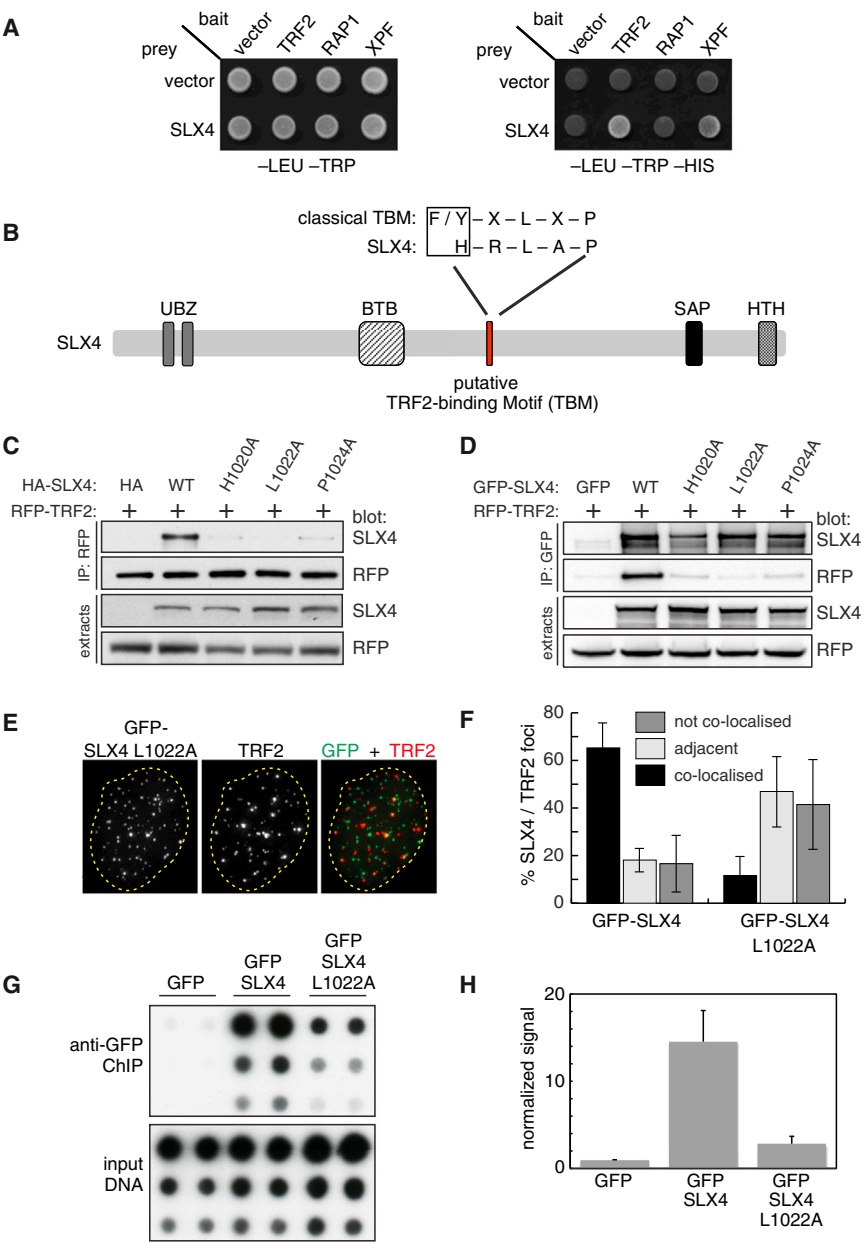

Figure 3. A TRF2-Binding Motif in SLX4

(A) Yeast two hybrid analysis was performed with a GAL4 activation domain (GAD) fusion of SLX4 and GAL4 DNA binding domain (GBD) fusion of TRF2, RAP1, or XPF to detect interaction between these proteins. Cells grown on medium lacking LEU and TRP (to select for bait and prey plasmids) were replica plated to medium lacking LEU, TRP, and HIS to test for activation of the *HIS3* reporter gene.

(B) Schematic diagram of the modular domain organization of SLX4. The putative TBM is highlighted in red, and the sequence of the putative TBM from SLX4 is compared with the classical TRF2-binding motif (TBM).

(C) U2OS cells were cotransfected with RFP-tagged TRF2 and HA-tagged SLX4 wild-type (WT), or HA-SLX4 bearing alanine substitutions at H1020, L1022, or P1024. Vector expressing HA tag only was used as control. Cells were lysed and subjected to immunoprecipitation with anti-RFP antibodies, and precipitates were probed with the antibodies indicated.

(D) Same as (C) except that SLX4 was GFP tagged, and extracts were subjected to immunoprecipitation with anti-GFP antibodies.

(E) Indirect immunofluorescence analysis of U2OS cells stably expressing GFP-SLX4-L1022A. GFP-SLX4 or endogenous TRF2 foci were visualized.

(F) The proportion of foci in U2OS cells formed by GFP-SLX4 or GFP-SLX4-L1022A that cocolocalize with TRF2, that are adjacent to but not overlapping with TRF2, or that do not colocalize with TRF2 was quantitated.

(G) Telomere-ChIP analysis of GFP-SLX4 or GFP-SLX4-L1022A, or GFP only, stably expressed in U2OS cells. DNA from immunoprecipitates was subjected to 3-fold serial dilutions, before spotting onto Hybond N+ and hybridization with a radioactively labeled telomeric probe (upper panel) or an Alu DNA probe (lower panel). Input DNA prepared from cell extracts before immunoprecipitation was subjected to similar analysis. The "input DNA" lane shows 10%, 3%, and 1% of the total DNA in cell extract, respectively.

(H) The ChIP signal in the dots corresponding to each serial dilution for each immunoprecipitate in (G) was quantitated and added together. To normalize the hybridization signals, the resulting totals for each precipitate were divided by the total input signal (left panels).

See also Figures S2 and S3.

wild-type HA-SLX4 coprecipitated with RFP-TRF2, mutation of H1020, L1022, or P1024 caused a major reduction in the amount of HA-SLX4 coprecipitating with RFP-TRF2 (Figure 3C). Similar results were obtained when GFP-tagged SLX4 was immunoprecipitated from cells coexpressing RFP-TRF2 (Figure 3D). Importantly, mutating H1020, L1022, or P1024 had no effect on the ability of SLX4 to interact with XPF-ERCC1, MUS81, or SLX1 (Figure S2A). Taken together, these data show that a TBM in human SLX4 mediates interaction with TRF2. Intriguingly, a clear TBM is found in SLX4 in primates but not in mammals lower down the evolutionary tree (Figure S2B). SLX4 orthologs in some mammals have a motif that is vaguely similar to the TBM in primates (Figure S2B), but none of the mammalian motifs would be expected to interact with TRF2 based on previous work (Chen et al., 2008).

The SLX4 Complex Is Recruited to Telomeres by TRF2 in Human Cells

We next tested if mutating the TBM in SLX4 affects its localization at telomeres. To this end, GFP-tagged wild-type SLX4, or GFP-SLX4-L1022A, was stably expressed in U2OS cells and foci were analyzed. Surprisingly, the overall number of foci formed by the SLX4 L1022A mutant was similar to wild-type SLX4 (Figures 3E and 3F). However, whereas almost 65% of wild-type GFP-tagged SLX4 foci colocalized with TRF2, only around 10% of foci formed by the SLX4 L1022A mutant

coincided with TRF2, and more than 40% of the foci clearly did not (Figures 3E and 3F). The remaining 40% of SLX4–L1022A foci did not colocalize with TRF2, but were found adjacent to, but distinct from TRF2 foci (Figures 3E and 3F). To further test the impact of mutating the SLX4 TBM on telomere binding, we used ChIP analysis, which revealed that mutating SLX4 L1022 to alanine caused an almost 80% reduction in the amount of telomeric DNA associated with SLX4 (Figures 3G and 3H). These data suggest that TRF2 is required for localizing SLX4 at telomeres. We tested this idea further using a dominant-negative form of TRF2 (TRF2ΔBΔM) that heterodimerizes with endogenous TRF2 blocking its binding to DNA (van Steensel et al., 1998). As shown in Figure S2C, overexpression of an RFP-tagged form of TRF2ΔBΔM, but not wild-type TRF2, caused a substantial reduction in the number of SLX4 foci in U2OS cells (Figure S2C). Some of the cells transfected with TRF2ΔBΔM did not express this protein, and SLX4 foci were normal in these cells (Figure S2C). Taken together, these data indicate that TRF2 recruits SLX4 to telomeres in human cells.

We also tested if the SLX4-TRF2 interaction is required for association of SLX1 with telomeres. We showed earlier that endogenous SLX1 forms TRF2-coincident foci in cells overexpressing wild-type SLX4 (Figure 1D). SLX1 also forms foci in cells overexpressing SLX4-L1022A, but, although these foci colocalize with SLX4-L1022A, they do not colocalize with TRF2 (Figure S3A). This experiment shows that SLX1 is recruited to telomeres by SLX4.

SLX4 Localizes at and Repairs DNA Damage Independently of TRF2

SLX4 is required for efficient DNA repair. Because TRF2 has been shown to localize at sites of DNA damage (Huda et al., 2012), and to promote DNA repair (Huda et al., 2009), we tested the possibility that TRF2 might recruit SLX4 to DNA damage sites as well as to telomeres. To this end, we induced DNA damage using local laser microirradiation and then checked by confocal microscopy for the ability of SLX4 to form "laser stripes." Time-lapse experiments revealed that GFP-tagged SLX4 formed subnuclear stripes along the track of DNA damage induced by laser irradiation visible within 12 min of irradiation, reaching a maximum intensity after 1 hr (Figure S3B). The SLX4-L1022A mutant localized at tracks of laser-induced DNA damage with similar kinetics and intensity to wild-type SLX4 (Figure S3B). We conclude from these data that TRF2 is not required to localize SLX4 at sites of DNA damage.

We also tested if the association of SLX4 with TRF2 is required for DNA repair using genotoxin hypersensitivity as readout. To this end, we stably expressed untagged forms of SLX4 and SLX4-L1022A in cells from Fanconi anemia patient EUFA-1354 that express abnormally low levels of an N-terminally truncated form of SLX4 (Stoepker et al., 2011). Empty vector was used as control. As shown in Figure S3C, wild-type SLX4 and SLX4-L1022A are indistinguishable in their ability to rescue the mitomycin-C hypersensitivity of EUFA-1354 cells. Taken together, the data above indicate that neither the localization of SLX4 at DNA damage sites, nor the ability of SLX4 to promote DNA repair, requires binding to TRF2.

Localization-Dependent and -Independent Roles for SLX4 in Promoting Telomere Homeostasis

We next tested if preventing localization of SLX4 at telomeres affects telomere function. Because the L1022A SLX4 mutant interacts with XPF-ERCC1, MUS81-EME1, and SLX1 (Figure S2A) but does not localize at telomeres (Figures 3E–3H), we reasoned that it might function as a dominant negative by sequestering the associated nucleases away from telomeres. In this light, we made U2OS cells that stably express GFP-tagged SLX4, or GFP-SLX4-L1022A in a tetracycline-inducible manner. Upon induction of SLX4-L1022A, we noticed an increase in the proportion of cells with "TIFs" (telomere dysfunction-induced foci) (Takai et al., 2003), defined as 53BP1 foci that colocalize with TRF1, compared with cells expressing wild-type SLX4 (Figure 4A). In contrast, there was little difference between wild-type SLX4 and the SLX4-L1022A mutant in terms of the induction of 53BP1 foci that did not colocalize with TRF1 (Figure 4A). This experiment argues that failure to properly target SLX4 to telomeres causes telomere damage. Consistent with these data, siRNA-mediated depletion of SLX4 from U2OS cells increased the proportion of cells with TIFs (Figures S4A and S4B). SLX4-specific siRNAs 3 and 4 resulted in more efficient depletion of SLX4 than siRNAs 1 and 2, and consequently they were more potent at inducing TIFs.

Intriguingly, the lack of an obvious TRF2 binding motif in nonprimate mammalian orthologs of SLX4 suggests that SLX4 should not localize at telomeres in mouse cells, for example, and we next investigated this possibility. As shown in Figure S4C, whereas human SLX4 forms foci that colocalize with TRF2 when ectopically expressed in mouse embryonic fibroblasts (MEFs), mouse SLX4 forms foci but they do not colocalize with TRF2. This is reminiscent of the human SLX4-L1022A mutant that forms foci that do not colocalize with telomeres (Figure 3E–3H). These observations indicate that SLX4 does not associate stably with telomeres in mouse cells, at least in fibroblasts. Nonetheless, we reasoned that SLX4 might have roles at telomeres that do not require stable association with chromosome ends. With this in mind, we analyzed telomeres in *Slx4*$^{-/-}$ mice generated in this laboratory, which will be described in detail elsewhere (D.C., N. Nair, A.C. Declais, C. Lachaud, R.T., T.J. Macartney, D.M.J. Lilley, J.S.C. Arthur, and J.R., unpublished data). Analysis of organs and cells from these mice revealed a number of telomere defects. First, we observed increased incidence of TIFs in mouse embryonic fibroblasts (MEFs) from *Slx4*$^{-/-}$ mice (Figure S4D). Second, telomeres in livers from *Slx4*$^{-/-}$ mice were longer than in *Slx4*$^{+/-}$ mice or wild-type mice (Figure 4B). Telomeres were also longer in MEFs from *Slx4*$^{-/-}$ mice, but lengthening was reversed by expression of mouse SLX4 in these cells so that telomeres were similar in length to wild-type MEFs (Figure 4C). These data suggest that SLX4 might play a role in trimming telomeres to prevent overlengthening. We also found that telomeres from *Slx4*$^{-/-}$ MEFs show increased fragility assessed by the frequency of multitelomeric signals (MTSs) compared with *Slx4*$^{+/-}$ MEFs and wild-type cells (Figure 4D). The data above indicate that targeting of SLX4 to telomeres prevents DNA damage in human cells, and that SLX4 also plays a role in telomere homeostasis in mice in a manner that does not appear to require the stable retention of the SLX4 complex at telomeres.

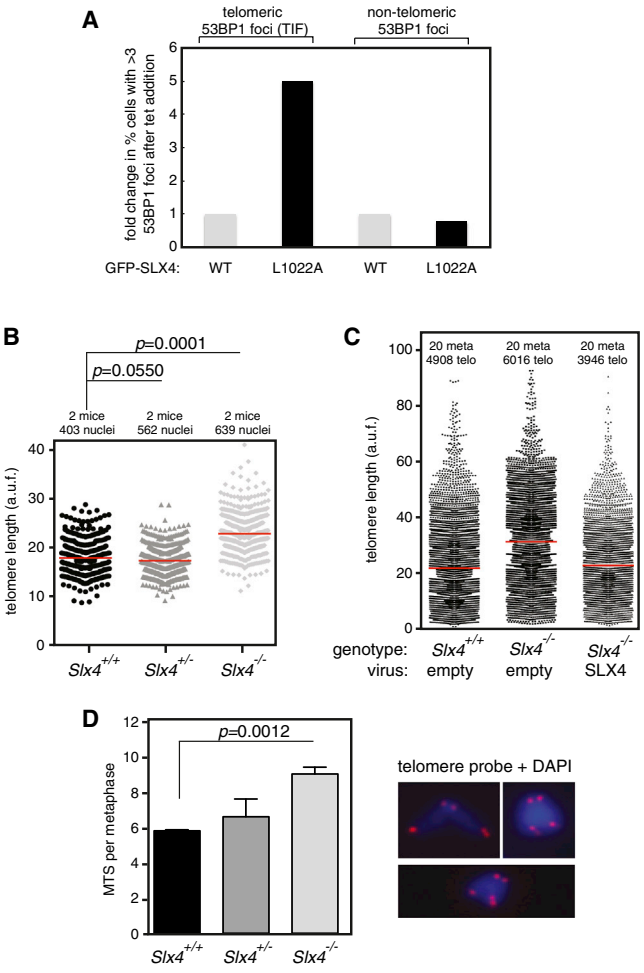

Figure 4. Localization-Dependent and -Independent Roles of SLX4 in Regulating Telomere Homeostasis

(A) U2OS cells stably expressing tetracycline-inducible forms of GFP-SLX4 wild-type (WT) or GFP-SLX4-L1022A were incubated, or not, with tetracycline for 48 hr to induce maximal protein expression. Cells were fixed and subjected to immunofluorescence analysis of 53BP1 foci and TRF1 foci. The proportion of cells with greater than three 53BP1 foci that colocalized with TRF1 ("telomeric"), and that did not colocalize with TRF1 ("nontelomeric") was counted before and after addition of tetracycline. The fold change after addition of tetracycline was calculated. At least 200 cells were counted for each condition, in two independent experiments.

(B) Telomere fluorescence distribution of individual telomere dots in paraffin-embedded liver sections of mice of the indicated genotype as determined by q-FISH analysis. Mean fluorescence is indicated by the red horizontal line; a.u.f., arbitrary units of fluorescence. The total numbers of mice and nuclei analyzed per genotype are indicated. The Wilcoxon-Mann-Whitney rank sum test was used for statistical comparison; p values are indicated.

(C) Telomere fluorescence distribution of individual telomere dots in MEFs from wild-type mice or *Slx4*$^{-/-}$ mice stably expressing mouse SLX4, as determined by q-FISH analysis. Empty vector was used as control. Mean fluorescence is indicated by the red horizontal line; a.u.f., arbitrary units of fluorescence. The total numbers of metaphase spreads ("meta"), and telomeres ("telo") analyzed per genotype are indicated.

(D) Frequency of multitelomeric signals (MTSs) per metaphase in primary MEFs of the indicated genotypes. Data are presented as mean and SEM. Representative images of MTSs are shown. The Wilcoxon-Mann-Whitney rank sum test was used for statistical comparison; p values are indicated.

See also Figures S3 and S4.

DISCUSSION

In this study, we showed SLX4 is recruited to telomeres in human cells by TRF2. We identified a motif in human SLX4 required for direct interaction with TRF2 that is similar but not identical to the TRF2-binding motif (TBM; F/Y-X-L-X-P) identified in proteins such as Apollo (Chen et al., 2008). In the SLX4 motif, however, the F/Y residue is replaced by a histidine residue. This observation extends the consensus TRF2-binding motif and raises the possibility that other proteins might interact with TRF2 through TBMs similar to that of SLX4. Although SLX4 is a rapidly evolving protein, it is somewhat surprising that the SLX4 TBM-like motif is conserved in primates but not in mammals lower down the evolutionary tree (Figure S2B). The absence of a TBM, however, does not exclude the possibility that SLX4 (or an SLX4-associated protein) in nonprimate species associates with TRF2 and/or telomeres by alternative mechanisms. However, we have been unable to detect endogenous SLX4 at telomeres in mouse embryonic fibroblasts, and, whereas human SLX4 overexpressed in MEFs forms telomeric foci, mouse SLX4 does not (Figure S4C). Therefore, SLX4 associates with TRF2 and telomeres in primates but not in other mammals. In human cells, preventing localization of SLX4 at telomeres caused signs of DNA damage (Figure 4A). The precise nature of this damage is not yet clear, but it might result from difficulties in one of the many processing steps during and after DNA replication necessary for establishing the correct structure at telomeres.

It appears that not all of the telomere-related functions of the SLX4 complex require stable association with telomeres, because telomeres are longer and more fragile in organs and cells from *Slx4*$^{-/-}$ mice and telomere lengthening in *Slx4*$^{-/-}$ MEFs can be reversed by expression of wild-type SLX4 (Figures 4B and 4C). From this perspective, SLX4 might mediate "telomere trimming," a mechanism that has been proposed to prevent overlengthening of telomeres (Pickett and Reddel, 2012). It is not yet clear which of the SLX4-associated nucleases are required to prevent telomere lengthening. It is unlikely that XPF-ERCC1 is the relevant nuclease because telomere length is not affected in *Ercc1*$^{-/-}$ mice (Zhu et al., 2003). The nuclease that promotes SLX4-dependent telomere shortening could be MUS81-EME1 and/or SLX1; it will be interesting to test the relevant knockout mice for abnormally long telomeres. SLX1 is a good candidate considering the Boulton lab has shown that it is required for the production of T circles in cells lacking RTEL1 (Vannier et al., 2012). The consequences of overlong telomeres for cell function and organism function are not clear, but this will be interesting to study.

EXPERIMENTAL PROCEDURES

Immunofluorescence Analysis

U2OS cells expressing GFP-SLX4 were preextracted in CSK buffer: 10 mM PIPES (pH 6.8) containing 100 mM NaCl, 300 mM sucrose, 3 mM magnesium chloride, 1 mM EGTA, and 0.5% [v/v] Triton X-100, fixed with 2% paraformaldehyde (PFA) (pH 7.0), permeabilized with PBS containing 0.5% (v/v) Triton X-100, blocked with BSA (3% w/v) in PBS, and probed with primary antibodies for 1 hr at room temperature. After extensive washing, cells were incubated with secondary Alexa antibodies for 2 hr at room temperature. Cells were

stained with DAPI before mounting on glass slides. Wide-field image stacks of cells were acquired using a Deltavision microscope (Applied Precision) and subjected to iterative deconvolution to remove out-of-focus light and were further processed in OMERO (Allan et al., 2012). For endogenous SLX4 immunofluorescence, cells grown on poly-L-lysine-coated coverslips were preextracted in CSK buffer or PBS containing 0.5% Triton X-100 prior to fixation in 3% PFA in CSK (pH 7.0). Cells were permeabilized in PBS-containing 0.5% (v/v) Triton X-100 and then blocked in antibody dilution buffer (AbDil): PBS containing 5% normal donkey serum, 0.1% fish skin gelatin, 0.1% Triton X-100, 0.05% Tween-20, and 0.05% sodium azide, before incubation with primary antibodies in AbDil for 1 hr at room temperature or overnight at 4°C. After washing, cells were incubated with the relevant secondary antibodies for 2 hr at room temperature, stained with DAPI, and mounted on glass slides.

Chromatin Immunoprecipitation

Cells grown to subconfluency on 15 cm plates were crosslinked with 1% (v/v) formaldehyde for 15 min, with 0.125 M glycine for 5 min, and then washed twice with PBS. Cells (4×10^6 cells per IP) were lysed in chromatin immunoprecipitation (ChIP) lysis buffer (1% SDS, 10 mM EDTA, 50 mM Tris-HCl [pH 8.0] plus protease inhibitors), followed by sonication for 15 s at 50% amplitude and 30 s rest; this was repeated eight times at 4°C before cells were centrifuged at 12,000 rpm at 4°C for 10 min. Cell supernatants were diluted 1:10 in ChIP dilution buffer (1% [v/v] Triton X-100, 2 mM EDTA, 150 mM NaCl, and 20 mM Tris-HCl [pH 8.0]) and precleared with 2 μg of sheared salmon sperm DNA (Invitrogen) and 20 μl protein G-Sepharose beads per equivalent IP volume (2 ml). The supernatant was incubated with the relevant antibodies overnight, before the addition of protein G-Sepharose beads for 1 hr. After extensive washes, immune complexes were eluted with elution buffer (100 mM $NaHCO_3$ and 1% SDS) and incubated overnight at 65°C to reverse crosslinks. Protein and RNA were removed by incubation with proteinase K and RNase A at 37°C for 1 hr. DNA was purified by extraction with phenol/chloroform/isoamyl alcohol (25:24:1), followed by centrifugation and retrieval of the aqueous supernatant. DNA was precipitated with ice-cold ethanol (96% v/v), washed with 70% ethanol, and resuspended in 100 μl of water. Dot blotting and hybridization of ChIP are described in the Supplemental Information.

Full details of all other experimental procedures are given in the Extended Experimental Procedures.

SUPPLEMENTAL INFORMATION

Supplemental Information includes Extended Experimental Procedures and four figures and can be found with this article online at http://dx.doi.org/10.1016/j.celrep.2013.07.033.

ACKNOWLEDGMENTS

We are grateful to James Hastie, Hilary MacLauchlan, and the Antibody Production Team at Division of Signal Transduction Therapy, University of Dundee for help with antibody production, and to DNA Sequencing Service at CLS, University of Dundee. We are grateful to the Centre for High resolution Image Processing (CHIP) and Christophe Lachaud in the Rouse lab for help with microscopy, and to Steve West for the gift of antibodies against TRF2. We are grateful to Johan de Winter for the gift of EUFA-1354 SLX4-defective Fanconi anemia cells. We are grateful to Saskia Hutten for CCL-211 cells. We thank members of J.R.'s laboratory for critically reading the manuscript, and we thank Ivan Muñoz for help with image processing. J.S.J.W. is a Wellcome Trust Clinical Fellow. M.A.B.'s laboratory is funded with the Spanish Ministry of Science and Innovation, projects SAF2008-05384 and 2007-A-200950 (TELOMARKER), European Research Council Advanced grant GA#232854, the Körber Foundation, Fundación Botín, and Fundación Lilly. Work in J.R.'s laboratory is supported by the Medical Research Council (MRC), and by the pharmaceutical companies supporting the Division of Signal Transduction Therapy Unit (AstraZeneca, Boehringer-Ingelheim, GlaxoSmithKline, Merck KgaA, Janssen Pharmaceutica, and Pfizer) associated with the MRC PPU.

Received: June 5, 2013
Revised: July 10, 2013
Accepted: July 25, 2013
Published: August 29, 2013

REFERENCES

Allan, C., Burel, J.M., Moore, J., Blackburn, C., Linkert, M., Loynton, S., Macdonald, D., Moore, W.J., Neves, C., Patterson, A., et al. (2012). OMERO: flexible, model-driven data management for experimental biology. Nat. Methods *9*, 245–253.

Andersen, S.L., Bergstralh, D.T., Kohl, K.P., LaRocque, J.R., Moore, C.B., and Sekelsky, J. (2009). Drosophila MUS312 and the vertebrate ortholog BTBD12 interact with DNA structure-specific endonucleases in DNA repair and recombination. Mol. Cell *35*, 128–135.

Blasco, M.A. (2007). Telomere length, stem cells and aging. Nat. Chem. Biol. *3*, 640–649.

Bryan, T.M., Englezou, A., Gupta, J., Bacchetti, S., and Reddel, R.R. (1995). Telomere elongation in immortal human cells without detectable telomerase activity. EMBO J. *14*, 4240–4248.

Cesare, A.J., and Reddel, R.R. (2010). Alternative lengthening of telomeres: models, mechanisms and implications. Nat. Rev. Genet. *11*, 319–330.

Chen, Y., Yang, Y., van Overbeek, M., Donigian, J.R., Baciu, P., de Lange, T., and Lei, M. (2008). A shared docking motif in TRF1 and TRF2 used for differential recruitment of telomeric proteins. Science *319*, 1092–1096.

Déjardin, J., and Kingston, R.E. (2009). Purification of proteins associated with specific genomic Loci. Cell *136*, 175–186.

Fekairi, S., Scaglione, S., Chahwan, C., Taylor, E.R., Tissier, A., Coulon, S., Dong, M.Q., Ruse, C., Yates, J.R., 3rd, Russell, P., et al. (2009). Human SLX4 is a Holliday junction resolvase subunit that binds multiple DNA repair/recombination endonucleases. Cell *138*, 78–89.

Greider, C.W., and Blackburn, E.H. (1989). A telomeric sequence in the RNA of Tetrahymena telomerase required for telomere repeat synthesis. Nature *337*, 331–337.

Huda, N., Tanaka, H., Mendonca, M.S., and Gilley, D. (2009). DNA damage-induced phosphorylation of TRF2 is required for the fast pathway of DNA double-strand break repair. Mol. Cell. Biol. *29*, 3597–3604.

Huda, N., Abe, S., Gu, L., Mendonca, M.S., Mohanty, S., and Gilley, D. (2012). Recruitment of TRF2 to laser-induced DNA damage sites. Free Radic. Biol. Med. *53*, 1192–1197.

Kim, Y., Lach, F.P., Desetty, R., Hanenberg, H., Auerbach, A.D., and Smogorzewska, A. (2011). Mutations of the SLX4 gene in Fanconi anemia. Nat. Genet. *43*, 142–146.

Lee, M.E., Rha, S.Y., Jeung, H.C., Kim, T.S., Chung, H.C., and Oh, B.K. (2008). Variation of the 3′ telomeric overhang lengths in human cells. Cancer Lett. *264*, 107–118.

Mocellin, S., Pooley, K.A., and Nitti, D. (2013). Telomerase and the search for the end of cancer. Trends Mol. Med. *19*, 125–133.

Muñoz, I.M., Hain, K., Déclais, A.C., Gardiner, M., Toh, G.W., Sanchez-Pulido, L., Heuckmann, J.M., Toth, R., Macartney, T., Eppink, B., et al. (2009). Coordination of structure-specific nucleases by human SLX4/BTBD12 is required for DNA repair. Mol. Cell *35*, 116–127.

Neumann, A.A., Watson, C.M., Noble, J.R., Pickett, H.A., Tam, P.P., and Reddel, R.R. (2013). Alternative lengthening of telomeres in normal mammalian somatic cells. Genes Dev. *27*, 18–23.

Palm, W., and de Lange, T. (2008). How shelterin protects mammalian telomeres. Annu. Rev. Genet. *42*, 301–334.

Pickett, H.A., and Reddel, R.R. (2012). The role of telomere trimming in normal telomere length dynamics. Cell Cycle *11*, 1309–1315.

Saito, T.T., Youds, J.L., Boulton, S.J., and Colaiácovo, M.P. (2009). Caenorhabditis elegans HIM-18/SLX-4 interacts with SLX-1 and XPF-1 and maintains genomic integrity in the germline by processing recombination intermediates. PLoS Genet. *5*, e1000735.

Stoepker, C., Hain, K., Schuster, B., Hilhorst-Hofstee, Y., Rooimans, M.A., Steltenpool, J., Oostra, A.B., Eirich, K., Korthof, E.T., Nieuwint, A.W., et al. (2011). SLX4, a coordinator of structure-specific endonucleases, is mutated in a new Fanconi anemia subtype. Nat. Genet. *43*, 138–141.

Svendsen, J.M., Smogorzewska, A., Sowa, M.E., O'Connell, B.C., Gygi, S.P., Elledge, S.J., and Harper, J.W. (2009). Mammalian BTBD12/SLX4 assembles a Holliday junction resolvase and is required for DNA repair. Cell *138*, 63–77.

Takai, H., Smogorzewska, A., and de Lange, T. (2003). DNA damage foci at dysfunctional telomeres. Curr. Biol. *13*, 1549–1556.

van Steensel, B., Smogorzewska, A., and de Lange, T. (1998). TRF2 protects human telomeres from end-to-end fusions. Cell *92*, 401–413.

Vannier, J.B., Pavicic-Kaltenbrunner, V., Petalcorin, M.I., Ding, H., and Boulton, S.J. (2012). RTEL1 dismantles T loops and counteracts telomeric G4-DNA to maintain telomere integrity. Cell *149*, 795–806.

Zeng, S., Xiang, T., Pandita, T.K., Gonzalez-Suarez, I., Gonzalo, S., Harris, C.C., and Yang, Q. (2009). Telomere recombination requires the MUS81 endonuclease. Nat. Cell Biol. *11*, 616–623.

Zhu, X.D., Niedernhofer, L., Kuster, B., Mann, M., Hoeijmakers, J.H.J., and de Lange, T. (2003). ERCC1/XPF removes the 3′ overhang from uncapped telomeres and represses formation of telomeric DNA-containing double minute chromosomes. Mol. Cell *12*, 1489–1498.